ON ESTIMATION OF COMPLIANCE FUNCTION OF A SOIL GROUND

Takuji Kobori (I)
Kaoru Kusakabe (II)
Presenting Author: K. Kusakabe

SUMMARY

The purpose of this paper is to estimate experimentally the compliance function of the rectangular foundation rest on a soil ground exciting by the vibration generator, and also, to discuss correspondence between theoretical and experimental results. From those results, it is found that the experimental compliance function does not well agree with the theoretical result for the elastic half-space, but very well agrees with that for the layered medium by reducing rigidity of soil medium near the boundary between soil and foundation.

INTRODUCTION

Since E. Reissner's paper (Ref. 1) on vibration problem of the circular foundation rest on a semi-infinite elastic medium, using the wave propagation theory, many investigators have developed analytically the compliance function, for various media, exciting directions, boundary conditions beneath the foundation and so on. On the other hand, there are few papers on estimation of the compliance function from experimental results (Ref. 3). Therefore, it is required to make clear correspondence of the theoretical compliance to the experimental one.

To detect experimentally the compliance function, the vibration test for reinforced concrete foundation was carried out by using an unbalanced rotating machine. The static and dynamic pressure distributions beneath the foundation, and the amplitude and phase characteristics at the top of the foundation were measured, and the dynamical ground compliance (compliance function) was calculated from those experimental results. The compliance function analyzed under the assumption that a soil ground consists of a semi-infinite elastic medium does not well agree with the experimental result. It is considered that rigidity of the soil ground near the surface around the foundation becomes smaller than that of the deeper soil medium during the vibration test. Because, soil medium has the nature that its rigidity is narrow linear region, and that it becomes smaller if the stress increases.

The compliance function of the rectangular foundation on two layered media is formulated, and the effect of small rigidity in the upper layer on the compliance function is discussed in this paper. The analytical compliance function for two layered media with small rigidity in the upper layer is compared with the experimental result, and is discussed their correspondence.

(I) Professor of Structural Engineering, Kyoto University, Kyoto, Japan

(II) Associated Professor of Structural Eng., Kobe University, Kobe, Japan

OUTLINE OF THE VIBRATION TEST

Vibration tests were carried out for five kinds of reinforced concrete foundations with various height at the campus of Kyoto University in Japan for a year from December, 1980 to December 1981. A profile of the ground at the site is shown in Fig.1. S-wave velocity V_S is 350m/sec, and P-wave velocity V_P is 650m/sec. From these velocities, Poisson's ratio $\nu = 0.3$ is calculated. Dimension of the foundation is 2.0m x 2.0m in the plan, and 35cm (CASE I), 70cm (CASE II), 105cm (CASE III), 140cm (CASE IV) and 200cm (CASE V) in height, shown in Fig.2 and Table. These foundation were constructed by adding new upper masses to the same base. The foundation was excited vertically and horizontally by means of an unbalanced rotating machine. The responses were measured at its top edge by some accelerometers, whose locations are shown by symbol N, S, E and W in Fig.2. Soil pressure gauges were set at the bottom of the foundation (Fig.3).

EXPERIMENTAL COMPLIANCE FUNCTION

The experimental compliance function can be calculated from the resultant amplitude and phase characteristics of the foundation.

Vertical Excitation

The equation of motion for the soil-foundation system can be written as

$$m\ddot{w} + \frac{1}{J_{1V} + iJ_{2V}} w = P_V e^{i\omega t} \qquad \cdots\cdots (1)$$

where $J_V = J_{1V} + iJ_{2V}$: vertical compliance function
m : mass of the foundation
w : vertical displacement of the foundation
P_V: amplitude of the vertical exciting force
ω : angular frequency, t : time, $i = \sqrt{-1}$
Symbol $\dot{}$: derivative with respect to time t

When the resultant velocity amplitude A_V and phase θ_V of the foundation are known, its behavior $\dot{w}$ can be represented by

$$\dot{w} = A_V \exp\{i(\omega t - \theta_V)\} \qquad \cdots\cdots (2)$$

By substituting eq.(2) into eq.(1), the compliance function is obtained for each angular frequency;

$$J_{1V} = \frac{1}{\omega \Delta_V}\left(m\omega - \frac{\sin\theta_V}{A_V/P_V}\right)$$
$$J_{2V} = -\frac{1}{\omega \Delta_V}\frac{\cos\theta_V}{A_V/P_V} \qquad \cdots\cdots (3)$$

where $$\Delta_V = (m\omega)^2 - 2m\omega\frac{\sin\theta_V}{A_V/P_V} + \left(\frac{1}{A_V/P_V}\right)^2 \qquad \cdots\cdots (4)$$

Horizontal Excitation

The equation of motion for the soil-foundation system with respect to the horizontal translation u_0 at the bottom and rotation ϕ of the foundation can be written as

$$m\ddot{u}_0 + ma\ddot{\phi} + \frac{1}{J_{1H} + iJ_{2H}} u_0 = P_H e^{i\omega t}$$

$$(I+ma^2)\ddot{\phi}+ma\ddot{u}_0+\frac{1}{J_{1R}+iJ_{2R}}\phi=\ell P_H e^{i\omega t} \qquad \cdots\cdots (5)$$

where $J_H=J_{1H}+iJ_{2H}$: horizontal compliance function
$J_R=J_{1R}+iJ_{2R}$: rotational compliance function
m : mass of the foundation, I : inertia moment
a : height of the gravity center, ℓ : height of excitation

When the horizontal velocity amplitude A_H and phase θ_H, and the vertical velocity amplitude A_R and phase θ_R at the edge were measured in the horizontal vibration test, $\dot{u}_0$ and $\dot{\phi}$ are represented as follows;

$$\dot{u}_0=A_H\exp\{i(\omega t-\theta_H)\}-\frac{h}{b}A_R\exp\{i(\omega t-\theta_R)\}$$
$$\dot{\phi}=\frac{1}{b}A_R\exp\{i(\omega t-\theta_R)\} \qquad \cdots\cdots (6)$$

where b is half width of the foundation and h is height of the foundation. By substituting eq.(6) into eq.(5) the following expression can be obtained

$$J_{1H}=\frac{1}{\omega\Delta_H}\left[m\omega\{(\frac{A_H}{P_H})^2+\frac{h}{b}\frac{h-a}{b}(\frac{A_R}{P_H})^2-\frac{2h-a}{b}\frac{A_R}{P_H}\frac{A_H}{P_H}\cos(\theta_R-\theta_H)\}\right.$$
$$\left.-(\frac{A_H}{P_H}\sin\theta_H-\frac{h}{b}\frac{A_R}{P_H}\sin\theta_R)\right]$$
$$J_{2H}=-\frac{1}{\omega\Delta_H}\{(\frac{A_H}{P_H}\cos\theta_H-\frac{h}{b}\frac{A_R}{P_H}\cos\theta_R)-\frac{a}{b}m\omega\frac{A_R}{P_H}\frac{A_H}{P_H}\sin(\theta_R-\theta_H)\}$$
$$J_{1R}=\frac{1}{\omega\Delta_R}\left[\omega\{\frac{I-ma(h-a)}{b^2}(\frac{A_R}{P_H})^2+\frac{a}{b}m\frac{A_R}{P_H}\frac{A_H}{P_H}\cos(\theta_R-\theta_H)\}\right. \qquad \cdots\cdots (7)$$
$$\left.-\frac{\ell}{b}\frac{A_R}{P_H}\sin\theta_R\right]$$
$$J_{2R}=-\frac{1}{\omega\Delta_R}\left[m\omega\frac{a}{b}\frac{A_R}{P_H}\frac{A_H}{P_H}\sin(\theta_R-\theta_H)+\frac{\ell}{b}\frac{A_R}{P_H}\cos\theta_R\right]$$

where

$$\Delta_H=(m\omega)^2\{(\frac{A_H}{P_H})^2+(\frac{h-a}{b})^2(\frac{A_R}{P_H})^2-2\frac{h-a}{b}\frac{A_R}{P_H}\frac{A_H}{P_H}\cos(\theta_R-\theta_H)\}$$
$$-2m\omega\{\frac{A_H}{P_H}\sin\theta_H-\frac{h-a}{b}\frac{A_R}{P_H}\sin\theta_R\}+1$$
$$\Delta_R=\omega^2[\{\frac{I-ma(h-a)}{b}\}^2(\frac{A_R}{P_H})^2+(ma)^2(\frac{A_H}{P_H})^2 \qquad \cdots\cdots (8)$$
$$+2\frac{I-ma(h-a)}{b}ma\frac{A_R}{P_H}\frac{A_H}{P_H}\cos(\theta_R-\theta_H)]$$
$$-2\omega\ell\{\frac{I-ma(h-a)}{b}\frac{A_R}{P_H}\sin\theta_R+ma\frac{A_H}{P_H}\sin\theta_H\}+\ell^2$$

ANALYTICAL COMPLIANCE FUNCTION

The compliance function of two layered media is analyzed. The model of the ground consists of a semi-infinite elastic medium and an elastic layered medium with uniform depth rest on that medium as shown in Fig.4. The equation of motion for the isotropic homogeneous elastic medium is represented by

$$(\lambda+\mu)\{\frac{\partial\Delta}{\partial x},\frac{\partial\Delta}{\partial y},\frac{\partial\Delta}{\partial z}\}+\mu\nabla^2\{u,v,w\}=\rho\frac{\partial^2}{\partial t^2}\{u,v,w\} \qquad \cdots\cdots (9)$$

where $\{x,y,z\}=\{\frac{X}{B},\frac{Y}{B},\frac{Z}{B}\}$: Cartesian coordinates

$\{u,v,w\}=\{\frac{U}{B},\frac{V}{B},\frac{W}{B}\}$: displacement with respect to x,y and z

$$\Delta=\frac{\partial u}{\partial x}+\frac{\partial v}{\partial y}+\frac{\partial w}{\partial z},\qquad \nabla^2=\frac{\partial^2}{\partial x^2}+\frac{\partial^2}{\partial y^2}+\frac{\partial^2}{\partial z^2} \qquad \cdots\cdots (10)$$

λ, μ : Lamé's constants, t : time, ρ : density

By denoting Lamé's constants by λ_I, μ_I, density ρ_I, for the upper layered medium, and Lamé's constants by λ_{II}, μ_{II} and density ρ_{II}, for the layered medium and also, the depth of upper layered medium by D, the following relations are introduced from boundary condition that the displacement and stress at interface between the upper layer and the lower medium (z = d) are continued each other;

$$u_I = u_{II}, \quad v_I = v_{II}, \quad w_I = w_{II}, \quad \sigma_{zI} = \sigma_{zII}, \quad \tau_{xzI} = \tau_{xzII}, \quad \tau_{yzI} = \tau_{yzII} \quad \text{at } z = d \qquad \cdots\cdots (11)$$

Next, the boundary conditions on the surface (z = 0) are assumed by the following form;

(a) Vertical excitation

$$\sigma_z = \begin{cases} 0 & |x| > b, \text{ or } |y| > c \\ -q_V Q(t) & |x| \leq b, \text{ and } |y| \leq c \end{cases}, \quad \tau_{xz} = \tau_{yz} = 0 \qquad \cdots\cdots (12\text{-a})$$

(b) Horizontal excitation

$$\tau_{xz} = \begin{cases} 0 & |x| > b, \text{ or } |y| > c \\ -q_H Q(t) & |x| \leq b, \text{ and } |y| \leq c \end{cases}, \quad \sigma_z = \tau_{yz} = 0 \qquad \cdots\cdots (12\text{-b})$$

(c) Rotational excitation

$$\sigma_z = \begin{cases} 0 & |x| > b, \text{ or } |y| > c \\ -q_R (x/b) Q(t) & |x| \leq b, \text{ and } |y| \leq c \end{cases}, \quad \tau_{xz} = \tau_{yz} = 0 \qquad \cdots\cdots (12\text{-c})$$

By introducing the 3-dimensional Fourier transform with respect to x,y and t into eqs.(9)-(12), the following solutions can be obtaind.

(a) Vertical excitation

$$J_V = \frac{w_{ave}}{P_V} b\mu_I = \frac{a_0}{\pi^2} \int_0^\infty \frac{\xi\sqrt{\xi^2 - n_1^2}}{F(\xi)} T(\xi) \int_0^{\pi/2} S_V(a_0\xi, c/b, \theta)\, d\theta\, d\xi \qquad \cdots\cdots (13)$$

(b) Horizontal excitation

$$J_H = \frac{u_{ave}}{P_H} b\mu_I = \frac{a_0}{\pi^2} \int_0^\infty \left\{ \frac{\xi}{\sqrt{\xi^2 - 1}} \frac{U(\xi)}{L(\xi)} \int_0^{\pi/2} \sin^2\theta\, S_H(a_0\xi, c/b, \theta)\, d\theta + \frac{\xi\sqrt{\xi^2 - 1}}{F(\xi)} V(\xi) \int_0^{\pi/2} \cos^2\theta\, S_H(a_0\xi, c/b, \theta)\, d\theta \right\} d\xi \qquad \cdots\cdots (14)$$

(c) Rotational excitation

$$J_R = \frac{\phi_{ave}}{M_R} b^3\mu_I = \frac{a_0}{\pi^2} \int_0^\infty \frac{\xi\sqrt{\xi^2 - n_1^2}}{F(\xi)} T(\xi) \int_0^{\pi/2} S_R(a_0\xi, c/b, \theta)\, d\theta\, d\xi \qquad \cdots\cdots (15)$$

where, $P_V = 4bc\, q_V$, $P_H = 4bc\, q_H$, $M_R = \frac{4}{3} b^2 c\, q_R$

$$F(\xi) = F_1 \cosh\{(\alpha_1 + \alpha_2)a_0 d\} + F_2 \cosh\{(\alpha_1 - \alpha_2)a_0 d\} + F_3 \sinh\{(\alpha_1 + \alpha_2)a_0 d\} + F_4 \sinh\{(\alpha_1 - \alpha_2)a_0 d\} + F_5 \quad : \text{Rayleigh Function} \qquad \cdots (16)$$

$$F_1 = \{(2\xi^2 - 1)^2 - 4\xi^2\alpha_1\alpha_2\}[\{\xi^2 M^2 - \alpha_3\alpha_4 L^2\} - \alpha_1\alpha_2\{K^2 - 4\xi^2\alpha_3\alpha_4(\mu - 1)^2\}]$$
$$F_2 = -\{(2\xi^2 - 1)^2 + 4\xi^2\alpha_1\alpha_2\}[\{\xi^2 M^2 - \alpha_3\alpha_4 L^2\} + \alpha_1\alpha_2\{K^2 - 4\xi^2\alpha_3\alpha_4(\mu - 1)^2\}]$$
$$F_3 = -\{(2\xi^2 - 1)^2 - 4\xi^2\alpha_1\alpha_2\}(\alpha_1\alpha_4 + \alpha_2\alpha_3) n_s^2 \mu$$
$$F_4 = \{(2\xi^2 - 1)^2 + 4\xi^2\alpha_1\alpha_2\}(\alpha_1\alpha_4 - \alpha_2\alpha_3) n_s^2 \mu$$
$$F_5 = 8\xi^2\alpha_1\alpha_2(2\xi^2 - 1)\{KM - 2\alpha_3\alpha_4(\mu - 1)L\}$$

$$T(\xi) = T_1 \cosh\{(\alpha_1 + \alpha_2)a_0 d\} + T_2 \cosh\{(\alpha_1 - \alpha_2)a_0 d\} + T_3 \sinh\{(\alpha_1 + \alpha_2)a_0 d\} + T_4 \sinh\{(\alpha_1 - \alpha_2)a_0 d\} \qquad \cdots\cdots (17)$$

$$T_1 = (\alpha_1\alpha_4 + \alpha_2\alpha_3)n_s^2\mu, \quad T_3 = -\{\xi^2M^2 - \alpha_3\alpha_4L^2\} + \alpha_1\alpha_2\{K^2 - 4\xi^2\alpha_3\alpha_4(\mu-1)^2\}$$
$$T_2 = -(\alpha_1\alpha_4 - \alpha_2\alpha_3)n_s^2\mu, \quad T_4 = \{\xi^2M^2 - \alpha_3\alpha_4L^2\} + \alpha_1\alpha_2\{K^2 - 4\xi^2\alpha_3\alpha_4(\mu-1)^2\}$$

$$L(\xi) = \alpha_4 \cosh \alpha_2 a_0 d + \alpha_2\mu \sinh \alpha_2 a_0 d \quad : \text{Love Function} \quad \cdots (18)$$
$$U(\xi) = \alpha_2\mu \cosh \alpha_2 a_0 d + \alpha_4 \sinh \alpha_2 a_0 d$$
$$V(\xi) = T_1 \cosh\{(\alpha_1+\alpha_2)a_0 d\} - T_2 \cosh\{(\alpha_1-\alpha_2)a_0 d\} + T_3 \sinh\{(\alpha_1+\alpha_2)a_0 d\} - T_4 \sinh\{(\alpha_1-\alpha_2)a_0 d\}$$

$$K = 2\xi^2(\mu-1) + n_s^2, \quad L = 2\xi^2(\mu-1) - \mu, \quad M = 2\xi^2(\mu-1) + n_s^2 - \mu$$
$$\alpha_1^2 = \xi^2 - n_1^2, \quad \alpha_2^2 = \xi^2 - 1, \quad \alpha_3^2 = \xi^2 - n_2^2 n_s^2 \quad \alpha_4^2 = \xi^2 - n_s^2$$
$$n_1^2 = \left(\frac{V_{sI}}{V_{pI}}\right)^2, \quad n_2^2 = \left(\frac{V_{sII}}{V_{pII}}\right)^2, \quad n_s^2 = \left(\frac{V_{sI}}{V_{sII}}\right)^2$$
$$\mu = \mu_I/\mu_{II}, \quad d = D/B, \quad c = C/B, \quad b = B/B = 1, \quad c/b = C/B$$
$$a_0 = \omega B/V_{sI} : \text{nondimensional frequency}, \quad B : \text{reference length}$$

$$S_V(a_0\xi, c/b, \theta) = S_H(a_0\xi, c/b, \theta) = \left\{\frac{\sin(a_0\xi\cos\theta)}{a_0\xi\cos\theta}\ \frac{\sin(c/b\cdot a_0\xi\sin\theta)}{c/b\cdot a_0\xi\sin\theta}\right\}^2$$
$$S_R(a_0\xi, c/b, \theta) = \left[\frac{3}{c/b}\ \frac{\sin(a_0\xi\cos\theta)}{a_0\xi\cos\theta}\left\{\frac{\sin(c/b\cdot a_0\xi\sin\theta)}{(c/b\cdot a_0\xi\sin\theta)^2} - \frac{\cos(c/b\cdot a_0\xi\sin\theta)}{c/b\cdot a_0\xi\sin\theta}\right\}\right]^2 \quad \cdots\cdots (19)$$

and

$$w_{ave} = \int_{-c}^{c}\int_{-b}^{b} w(x,y,0)\,dx\,dy \Big/ \int_{-c}^{c}\int_{-b}^{b} dx\,dy$$
$$u_{ave} = \int_{-c}^{c}\int_{-b}^{b} u(x,y,0)\,dx\,dy \Big/ \int_{-c}^{c}\int_{-b}^{b} dx\,dy \quad \cdots\cdots (20)$$
$$\phi_{ave} = \int_{-c}^{c}\int_{-b}^{b} x\cdot w(x,y,0)\,dx\,dy \Big/ \int_{-c}^{c}\int_{-b}^{b} x^2\,dx\,dy$$

DISCUSSION OF RESULTS

The static pressure distribution at the bottom of the foundation is shown in Fig.5. The solid lines show the test results, and the dotted lines are the average stress calculated from weight of the foundation. It is found that, for all cases of the foundation, the stress at the edge is greater than that at its center. This is near Boussinesq distribution. The dynamic pressure distributions at the bottom of the foundation are shown in Figs.6-8. It is found from Fig.6 that, when the eccentric mass of the unbalanced rotating machine EM is small, the pressure distribution is rather uniform, but when EM becomes larger, it approaches Boussinesq distribution where the pressure is greater at the edge than at the center. Fig.7 shows the dynamic pressure distribution vs. the exciting frequency, for CASE V and EM = 10kg·cm. It is found from this figure that the pressure distribution is approximately uniform at the lower frequency, and approaches Boussinesq distribution at the higher frequency. The effect of weight of the foundation on the pressure distribution in the case of EM = 20kg·cm, f = 20Hz in frequency is shown in Fig.8. It is pointed out that the heavier the foundation, the greater the ratio of pressure at the edge to that at the center. Figs.9.10 and 11 show the experimental vertical, horizontal and rotational compliance function vs. the exciting frequency f, respectively. In these figures, the symbol ○ shows the compliance for CASE I, ● for CASE II, × for CASE III, △ for CASE IV and ▲ for CASE V. The real part of compliance becomes smaller, if the foundation becomes higher, but such tendency does not appear clearly in its imaginary part.

In the following, the experimental results are compared with the analytical ones. Fig.12 shows the velocity amplitude and phase characteristics of the

foundation (CASE Ⅲ) against frequency due to the vertical excitation with EM = 6kg·cm. The phase characteristics are denoted as the phase delay of the velocity response behind the exciting force. The symbol O shows the experimental results, while the solid line shows the analytical result for the elastic semi-infinite medium $V_S = 295^m/sec$, the broken line shows the analytical result for the two layered media, the ratio of the depth of the upper layer to the half width of the foundation, $d = 0.1$, the S-wave velocity $V_{SI} = 155^m/sec$ in the upper layered medium and $V_{SII} = 310^m/sec$ in the lower medium, and the dotted line for the two layered media, $d = 0.5$, $V_{SI} = 180^m/sec$ and $V_{SII} = 360^m/sec$. The S-wave velocities V_{SI} and V_{SII} are chosen under the following assumptions; first, it is assumed that the ratio of V_{SI} to V_{SII} is equal to $V_{SI}/V_{SII} = 0.5$ and secondary, it is to choose such wave velocity that the analytical resonant frequency of soil-foundation system coincides with the experimental one. In the case of the semi-infinite medium, the analytical and experimental resonant amplitudes do not agree with each other even if these resonant frequencies agree with each other. But if it is assumed that the layered depth $d = 0.5$, the analytical and experimental resonant amplitudes agree with each other. Figs.13 and 14 show the horizontal and vertical component of the amplitude and phase characteristics of the foundation (CASE Ⅲ) due to the horizontal excitation, respectively. For the layer depth $d = 0.2$, $V_{SI} = 130^m/sec$ and $V_{SII} = 260^m/sec$, the analytical and experimental results with each other. Comparison between the experimental compliance and the analytical one is shown in Figs.15,16 and 17, for the vertical, horizontal and rotational components, respectively. For the vertical compliance, the experimental result agrees very well with the analytical one in case of the layer depth $d = 0.5$. But for the horizontal and the rotational compliance, the experimental results do not coincide very well the analytical ones. Since the horizontal translation and rotation due to the horizontal excitation couple together, some errors will appear when these compliance are estimated.

CONCLUSION

In this paper, both the experimental and the analytical compliance functions are investigated, and it is pointed out that under the assumption reducing rigidity of soil medium near boundary between soil and foundation, both compliance functions coincide very well with each other. It will be required to study further on this assumption in the future.

ACKNOWLEDGMENT

The authors would like to thank to Dr. R. Minai, Professor of the Disaster Prevention Research Institute, Kyoto University, and Dr. K. Mizuhata, Professor of the Faculty of Engineering, Kobe University, for their helpful discussions.

REFERENCES

1) Reissner, E. : Stationäre, axialsymmetrishe, durch eine schüttelnde Masse erregte Schwingungen eines homogenen elastischen Halbraums, Ingeniur-Archiv, Vol.VII, 1936, pp.381-396.

2) Kobori, T., R. Minai and T. Suzuki : The Dynamical Ground Compliance of a Rectangular Foundation on a Viscoelastic Stratum, the Bulletin of the Disaster Prevention Research Institute, Kyoto University, Vol.20, 1971.

3) Kobori, T., K. Kusakabe and S. Setogawa : Dynamical Ground Compliance of Square Foundation on a Stiff Soil Ground, Proc. of International Symposium on Weak Rock, Tokyo, Japan, Sept., 1981, pp.1223-1228.

Table Specifications of the foundations

CASE		I	II	III	IV	V
height of the foundation	h (cm)	35.0	70.0	105.0	140.0	200.0
width of the foundation	2b (cm)	200.0	200.0	200.0	200.0	200.0
height of the gravity center	a (cm)	23.2	40.0	57.2	71.0	101.0
height of excitation	ℓ (cm)	63.0	98.0	133.0	162.0	222.0
weight of the foundation	W (t)	4.16	7.12	10.88	13.65	19.41
inertia moment	I ($t \cdot m^2$)	1.46	2.91	4.81	6.87	13.11

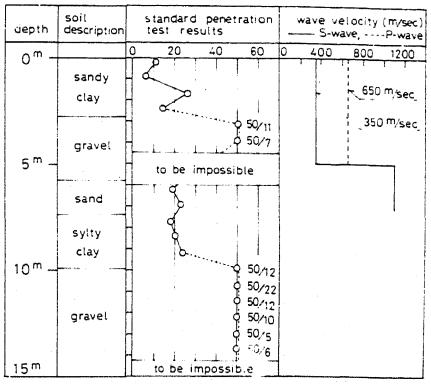

Fig. 1. Profile of the ground at the site

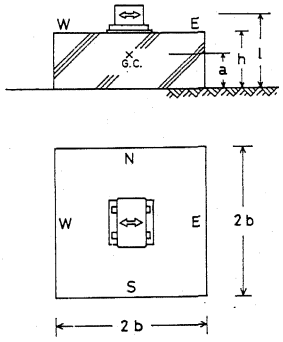

Fig. 2. Model of the foundation

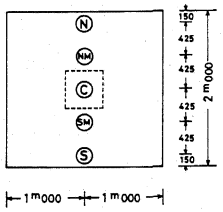

Fig. 3. Location of the pressure gauges

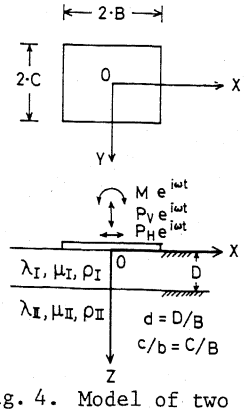

Fig. 4. Model of two layered media

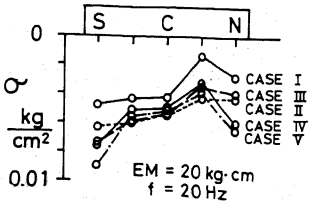

Fig. 8. Dynamic pressure distribution vs. weight

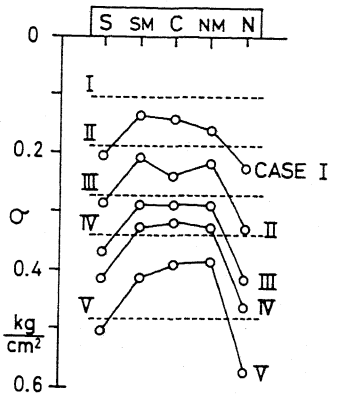

Fig. 5. Static pressure distribution

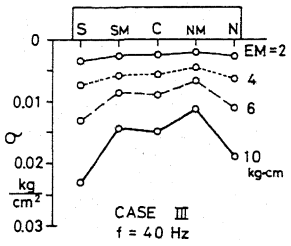

Fig. 6. Dynamic pressure distribution vs. eccentric mass

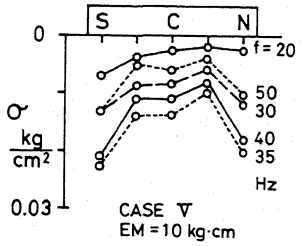

Fig. 7. Dynamic pressure distribution vs. frequency

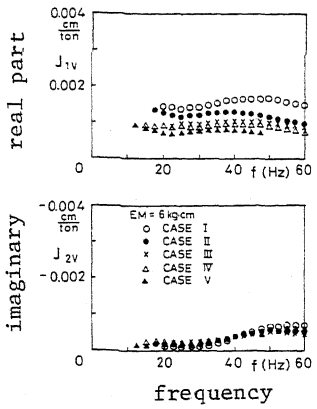

Fig. 9. Experimental vertical compliance

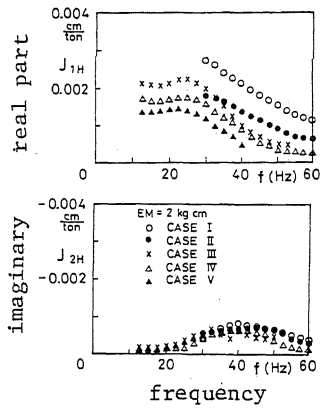

Fig.10. Experimental horizontal compliance

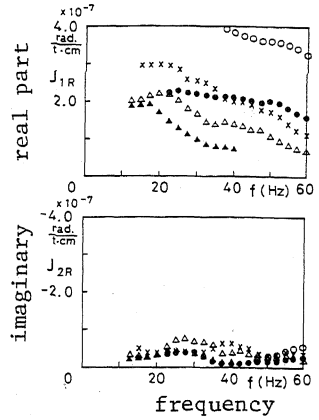

Fig.11. Experimental rotational compliance

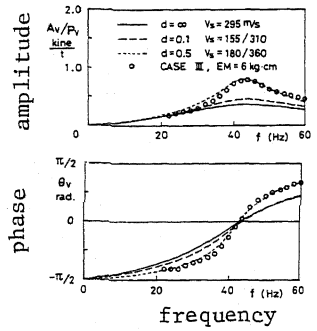

Fig.12. Vertical vibration characteristics to vertical exciting

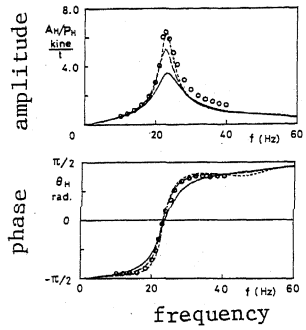

Fig.13. Horizontal vibration characteristics to horizontal exciting

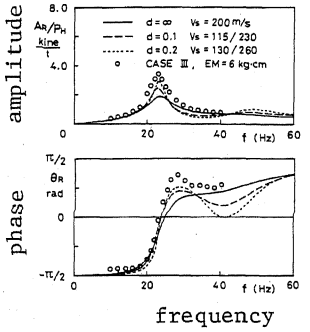

Fig.14. Vertical vibration characteristics to horizontal exciting

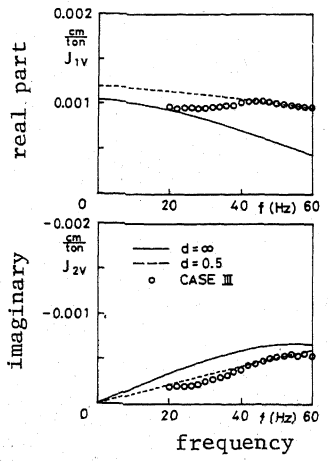

Fig.15. Comparison with vertical compliances

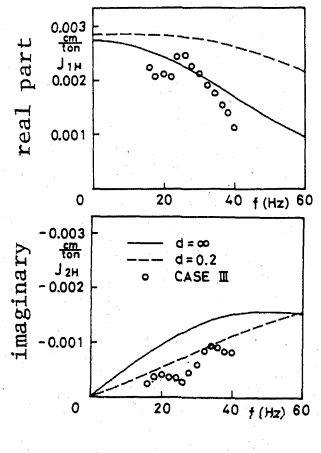

Fig.16. Comparison with horizontal compliance

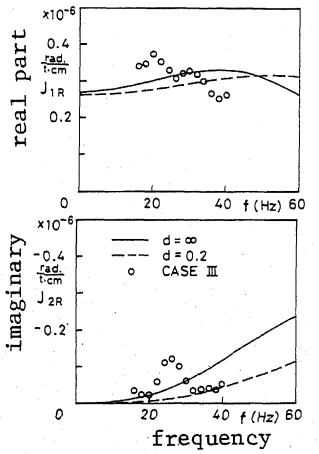

Fig.17. Comparison with rotational compliance